Nuclear Magnetic Resonance Solution Structure of the Peptidoglycan-Binding SPOR Domain from *Escherichia coli* DamX: Insights into Septal Localization

Kyle B. Williams,[†] Atsushi Yahashiri,[†] S. J. Ryan Arends,[†,‖] David L. Popham,[§] C. Andrew Fowler,*,[‡] and David S. Weiss*,[†]

[†]Department of Microbiology and [‡]NMR Core Facility, Carver College of Medicine, The University of Iowa, Iowa City, Iowa 52242, United States
[§]Department of Biological Sciences, Virginia Tech, Blacksburg, Virginia 24061, United States

S *Supporting Information*

ABSTRACT: SPOR domains are present in thousands of bacterial proteins and probably bind septal peptidoglycan (PG), but the details of the SPOR–PG interaction have yet to be elucidated. Here we characterize the structure and function of the SPOR domain for an *Escherichia coli* division protein named DamX. Nuclear magnetic resonance revealed the domain comprises a four-stranded antiparallel β-sheet buttressed on one side by two α-helices. A third helix, designated α3, associates with the other face of the β-sheet, but this helix is relatively mobile. Site-directed mutagenesis revealed the face of the β-sheet that

interacts with α3 is important for septal localization and binding to PG sacculi. The position and mobility of α3 suggest it might regulate PG binding, but although α3 deletion mutants still localized to the septal ring, they were too unstable to use in a PG binding assay. Finally, to assess the importance of the SPOR domain in DamX function, we constructed and characterized *E. coli* mutants that produced DamX proteins with SPOR domain point mutations or SPOR domain deletions. These studies revealed the SPOR domain is important for multiple activities associated with DamX: targeting the protein to the division site, conferring full resistance to the bile salt deoxycholate, improving the efficiency of cell division when DamX is produced at normal levels, and inhibiting cell division when DamX is overproduced.
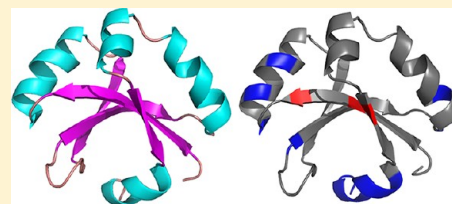
Bacterial cell division has been studied most intensively in *Escherichia coli*, where this process is mediated by a collection of ~30 proteins that localize to a structure at the midcell called the "septal ring" or "divisome" (reviewed in refs 1−3). Recently, several laboratories have shown that SPOR domain proteins are prominent components of the septal ring in a wide range of bacteria.[4−6] SPOR domains (Pfam 05036) are ~75 amino acids long and can be found in more than 5000 bacterial proteins in release 26 of the Pfam database.[7] These domains are called SPOR domains because the founding member of this family, a *Bacillus subtilis* cell wall amidase named CwlC, is a sporulation protein.[8] The available evidence suggests most SPOR domain proteins are involved in cell division.

SPOR domains have at least two noteworthy biological functions. The first is that they bind peptidoglycan (PG).[4,6,9] The second is that SPOR domains localize to the septal ring, even when artificially produced in heterologous bacteria.[4−6] Taken together, these observations imply SPOR domains localize to the division site by binding preferentially to septal PG. This would be a new mode of septal targeting as most bacterial division proteins are recruited to the septal ring via interactions with other division proteins. Although the chemical features of PG recognized by SPOR domains are still under investigation, mounting evidence suggests SPOR domains

target "naked" glycan strands generated by the action of amidases that remove stem peptides during biogenesis of the PG cell wall in the division septum.[5,9,10] Nevertheless, septal PG has not been shown to contain this or any other novel structure that would distinguish it from PG in the lateral wall or at the poles.[11−14] These considerations suggest that a molecular understanding of how SPOR domains bind (septal) PG will lead to new insights into PG metabolism during cell division.

Two SPOR domain structures have been published already, one from the *E. coli* cell division protein FtsN and the other from the *B. subtilis* sporulation protein CwlC.[15,16] These domains adopt a similar fold despite being only ~18% identical at the amino acid level. Each domain comprises a $\beta\alpha\beta\beta\alpha\beta$ secondary structure that assembles into a four-stranded antiparallel β-sheet buttressed on one side by two α-helices. This fold places SPOR domains in the ribonucleoprotein (RNP) fold superfamily, so-called because the first examples were RNA-binding domains from eukaryotic proteins involved in processing of mRNAs.[17−19] In the meantime, RNP folds have been identified in a wide range of proteins and shown to bind a wide range of ligands. As one example, the *E. coli* cell

division protein ZipA uses a modified RNP fold to bind the C-terminus of FtsZ.[20] In many RNP fold domains, including those from ZipA and the human RNA-binding protein U1A, the β-sheet serves as the primary binding surface for ligands.[17,20−23] How SPOR domains interact with PG is not known, although it has been suggested that the SPOR domain from CwlC binds glycan strands using two symmetrical sites comprising residues near the beginning of $\alpha 1$ and $\alpha 2$.[15]

We would like to know more about the SPOR−PG interaction and what role this plays in the biological function of SPOR domain proteins. Here we report the solution structure and some functional characterization of the SPOR domain from the DamX cell division protein of *E. coli*. Our choice of DamX reflected several considerations, starting with the fact that we expected to observe some new structural features because this SPOR domain is <20% identical to the SPOR domain from CwlC or FtsN, but DamX is interesting from a biological perspective, too. Although DamX clearly localizes to the septal ring, *damX* null mutants have no obvious division defect.[4,5] Nevertheless, deleting *damX* exacerbates the mild filamentation and chaining phenotypes caused by loss of another septal ring protein with a SPOR domain, DedD.[4,5] Conversely, deleting *damX* rescues growth of an *ftsQ1*(Ts) mutant at the nonpermissive temperature,[4] which is unexpected because combining mutations in septal ring proteins typically exacerbates division defects. Another noteworthy property of DamX is that, unlike most *E. coli* division proteins, it inhibits cell division when overproduced.[24] Finally, *damX* mutants are sensitive to bile salts, defective in invasion of host cells, and attenuated for induction of the MarA regulon needed for multidrug resistance.[4,25−27] These phenotypes suggest DamX may contribute to cell envelope biogenesis or integrity in ways that are distinct from the protein's role in cell division.

■ EXPERIMENTAL PROCEDURES

Media. For routine maintenance, cloning, and genetic analysis, *E. coli* strains were grown in Luria-Bertani medium with 10 g of NaCl per liter. When NaCl is omitted, the medium is termed LB0N. Ampicillin and kanamycin were used at concentrations of 200 and 40 μg/mL, respectively. Spectinomycin was used at a concentration of 100 μg/mL for plasmids and 35 μg/mL for chromosomal alleles. Isopropyl β-D-1-thiogalactopyranoside (IPTG) was used to induce gene expression at various concentrations as indicated in each experiment. To prepare isotopically labeled protein for nuclear magnetic resonance (NMR), cultures were grown in M9 minimal medium supplemented with B vitamins (1 mg/L), [U-13C]glucose (4 g/L), and 15NH4Cl (1 g/L). 15NH4Cl and [U-13C]glucose were obtained from Sigma.

Molecular Biology. Detailed descriptions of plasmid construction and mutagenesis are given in the Supporting Information, as are tables listing strains, plasmids, and primers (Tables S1−S3 of the Supporting Information). Polymerase chain reaction (PCR) was conducted with VENT DNA polymerase (New England Biolabs), and regions of plasmids derived by PCR were sequenced to verify their integrity. Localization studies of isolated SPOR domains were conducted using derivatives of Tat-targeted GFP (TTGFP) fusion vector pDSW962.[28] Expression plasmids for protein purification were derivatives of pQE80L (Qiagen). For some experiments, GFP fusions were introduced into the chromosome at the $\Phi 80$ attachment site using the CRIM vector system as described previously.[29]

Protein Purification. The hexahistidine-tagged (His6) DamX SPOR domain for PG binding assays and the His6-tagged DamX periplasmic domain for raising antibody were purified from cultures grown in LB essentially as described previously.[4] This procedure was modified to yield samples for NMR as follows. A 10 mL overnight culture of BL21(DE3) carrying a His6-DamXSPOR overproduction plasmid was grown in M9 containing glucose and ampicillin. The entire 10 mL was used to inoculate 1 L of M9 Amp containing 15NH4Cl and glucose (either unlabeled or 13C-labeled, as appropriate). The 1 L culture was grown at 30 °C for ~12 h until the OD600 reached 0.5; then protein production was induced by addition of IPTG to a final concentration of 1 mM, and the cultures were allowed to grow until the following morning (~12 h). Cells were harvested and proteins purified as described for inductions performed in LB except that the yield was only ~2 mg of protein per liter of culture.[4]

Typically, NMR spectra were collected using 0.7 mM protein in NMR buffer [50 mM potassium phosphate, 50 mM KCl (pH 6.5), 90% H2O, and 10% D2O]. To prepare samples, purified protein was dialyzed into 1.1× NMR buffer [55 mM potassium phosphate and 55 mM KCl (pH 6.5)], concentrated using a Microcon Centrifugal Filter device with a 3000 molecular weight cutoff (Millipore), and then diluted 10% by adding 1/10 volume of 99.9% D2O. For side chain and NOESY experiments not requiring detection of amide protons, an otherwise identical sample was exchanged into NMR buffer containing 99.9% D2O using a Microcon Centrifugal Filter device as described above. Samples of the wild-type SPOR domain proved to be stable for roughly 2 weeks, at which point fresh samples needed to be prepared.

NMR Spectroscopy. All NMR spectra were collected at 25 °C on a four-channel Varian UnityInova NMR spectrometer operating at 600 MHz and equipped with a triple-resonance PFG probe. Assignments were made using standard protein NMR methodology. Backbone resonances were assigned from HNCA, HN(CO)CA, HNCACB, CBCA(CO)NH, HNCO, and HN(CA)CO experiments. The side chain resonances were assigned using HCCH-TOCSY, C(CO)NH-TOCSY, H-(CCO)NH-TOCSY, HBHA(CBCACO)NH, and three-dimensional (3D) 15N TOCSY. Aromatic side chains were assigned using two-dimensional NOESY, TOCSY, and COSY experiments and connected to the rest of the molecule using (HB)CB(CGCD)HD and (HB)CB(CGCDCE)HE. Distance restraints were obtained from 3D 13C NOESY (140 and 200 ms) and 15N NOESY (100 and 200 ms) experiments. RDCs were measured for the backbone amides using an IPAP−15N HSQC experiment;[30] for the oriented sample, alignment was obtained using 5% PEG(C12E5)/hexanol bicelles[31] that gave a deuterium quadrupolar splitting of the HOD resonance of 25.2 Hz. Finally, backbone 15N T_1, 15N T_2, and {1H}−15N NOE relaxation parameters were measured.[32] Mixing times were 0, 22.1, 66.3, 132.6, 221.0 (twice), 442.0, 773.4, 1215.4, and 1767.9 ms for T_1; 12.9, 25.8, 51.6, 77.4 (twice), 103.2, 129.0, 154.8, 206.4, and 232.2 ms for T_2; and 0 and 3.5 s for NOE. All spectra were processed using NMRPipe.[33] RDC data and spectral overlays were analyzed using tools present in NMRPipe; relaxation rates were extracted using CurveFit,[34] and backbone and NOESY assignments were made using CCPN's Analysis software.[35] Order parameters were calculated and motional models for the SPOR domain residues determined according to the model free formalism[36,37] using Fast-Modelfree[38] to run ModelFree version 4.20.[34,39]
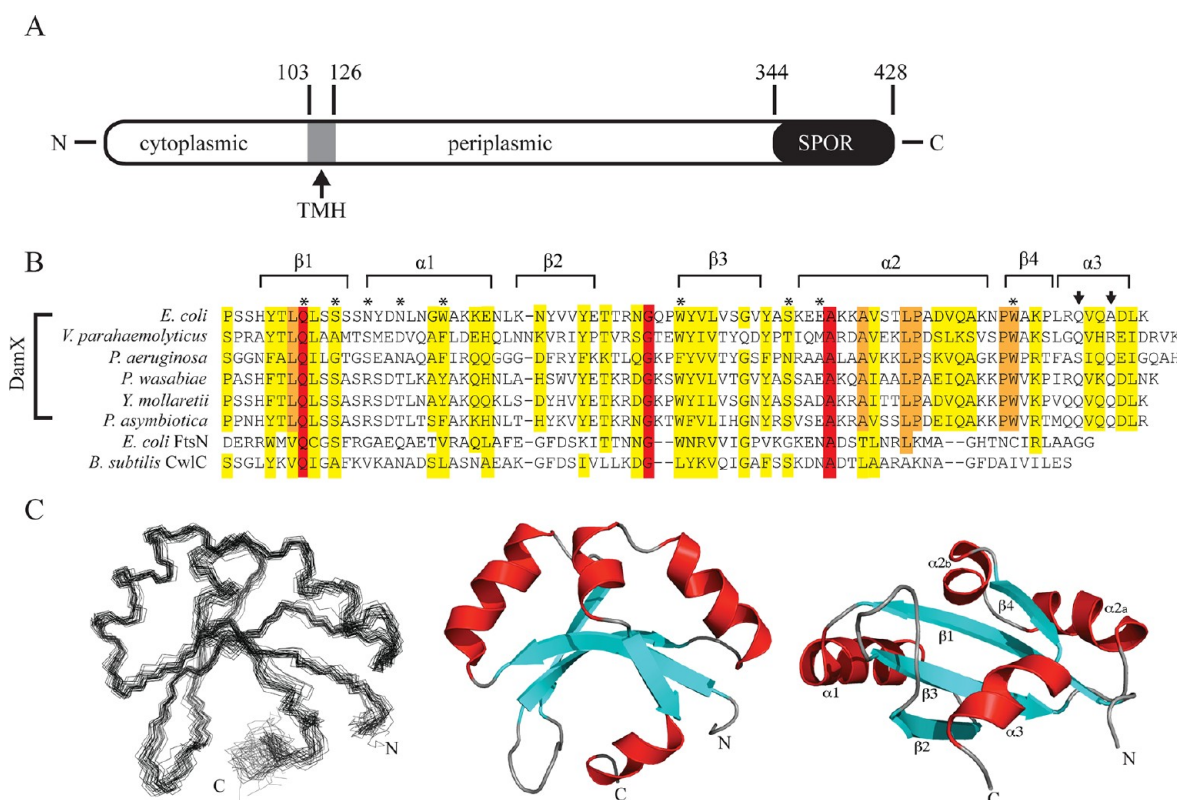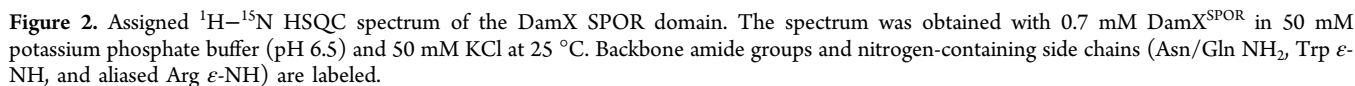
Figure 1. Structure of DamX and its SPOR domain. (A) Cartoon of DamX from *E. coli*. DamX is predicted to comprise a 103-amino acid cytoplasmic domain, a 23-amino acid transmembrane helix (TMH), and a 302-amino acid periplasmic domain, of which the last 84 amino acids constitute the SPOR domain. (B) Sequence alignment of SPOR domains of several DamX's with the SPOR domains from CwlC and FtsN. The secondary structure elements determined for the SPOR domain of DamX from *E. coli* are shown above the alignment. Asterisks denote residues mutated in this study. Arrows indicate the site of C-terminal truncations. The alignment was obtained using CLUSTAL W[54] with the following sequences: *E. coli* DamX residues 344−428, *Vibrio parahaemolyticus* DamX residues 417−505, *Pseudomonas aeruginosa* DamX residues 464−551, *Pectobacterium wasabiae* WPP163 residues 251−336, *Yersinia mollaretii* DamX residues 249−333, *Photorhabdus asymbiotica* DamX residues 232−316, *E. coli* FtsN residues 244−319, and *B. subtilis* CwlC residues 182−255. (C) Solution structure of the SPOR domain (DamX residues 344−428). Side-on view (left) of a backbone superposition of the 25 final structures. The average pairwise rsmd for residues is 0.795 Å. Side-on (middle) and bottom-up (right) views of a ribbon diagram of the domain, with β-strands colored blue, α-helices red, and loops gray. Note that α2 is interrupted by a proline.

Structure Calculations. All structure calculations were conducted using XPLOR-NIH.[40,41] Visualization and analysis of structures, as well as generation of figures, were conducted using both PyMOL[42] and UCSF Chimera.[43] Structure calculations began from an extended structure of the DamX construct. Initial structures were calculated using only those distance restraints that could be uniquely and unambiguously assigned, and the resulting structures were used to assign additional NOEs in an iterative manner. Dihedral angle restraints were obtained for backbone ϕ and ψ torsion angles using TALOS+[44] and assigned chemical shifts; flexible N-terminal residues as determined from relaxation analysis were excluded. Finally, RDC restraints were measured and implemented into later-stage structure calculations using the TENSOR module in XPLOR-NIH;[45] only those residues for which the RDCs could be unambiguously assigned, with minimal spectral overlap, and not in the flexible N-terminus were included. Force constants were ramped up during the structure calculations to the following final values: $k(vdW)$ = 4.0, $k(angles)$ = 1.0, $k(impr)$ = 1.0, $k(noe)$ = 20.0, $k(dihedral)$ = 200.0, and $k(RDC)$ = 1.0. A final ensemble of 250 structures was calculated, with the 25 lowest-energy structures accepted. NMR assignments and final coordinates were submitted to the

BioMagResBank and Protein Data Bank (PDB), entries 17783 and 2LFV, respectively.

Peptidoglycan Binding Assays. Binding of the His$_6$-DamX SPOR domain to PG sacculi was assayed by cosedimentation in an ultracentrifuge as described previously.[4] Whole PG sacculi for this assay were isolated and quantified by amino sugar analysis as described previously.[4] Routine PG binding assays used sacculi from wild-type strain EC251 harvested during exponential growth; the cells in such cultures are in various stages of the division cycle.

Localization of GFP Fusion Proteins by Fluorescence Microscopy. Live cells in the exponential growth phase were transferred to an agarose pad and visualized by fluorescence and phase contrast microscopy as described previously.[4] For ^{TT}GFP-DamX^{SPOR} constructs produced from plasmids, cultures were grown overnight in LB medium with 200 μg/mL ampicillin, then diluted 1:100 in the same medium, and grown for ∼4 h at 30 °C to reach an OD$_{600}$ of 0.5. The experiments were also conducted at 21 °C for some strains. GFP-DamX proteins produced from the chromosome were analyzed similarly except overnight cultures were diluted 1:500, antibiotic was omitted, and IPTG was used to induce expression (at the concentration indicated in each experiment).

Figure 2. Assigned $^{1}H-^{15}N$ HSQC spectrum of the DamX SPOR domain. The spectrum was obtained with 0.7 mM DamX^{SPOR} in 50 mM potassium phosphate buffer (pH 6.5) and 50 mM KCl at 25 °C. Backbone amide groups and nitrogen-containing side chains (Asn/Gln NH$_2$, Trp ε-NH, and aliased Arg ε-NH) are labeled.

Generation of the Antibody against DamX and Western Blotting. The polyclonal antiserum against the periplasmic domain of DamX was raised in New Zealand white rabbits. The protein antigen was raised against His$_6$-DamX (residues 122−428) overproduced in BL21 from pDSW1133 and purified by cobalt affinity chromatography. To reduce undesired cross-reactivity, the antiserum was cleaned up prior to its use by preabsorption against an extract from a Δ*damX* strain, EC1926. The preabsorbed antiserum was used at a dilution of 1:5000 for Western blotting, essentially as described previously.[4]

Deoxycholate Sensitivity. To assay for deoxycholate sensitivity, overnight cultures grown in LB were adjusted to an OD$_{600}$ of 0.01 in LB0N medium and then 5-fold serial dilutions were made and 3 μL aliquots were spotted onto an LB0N agar plate containing 0, 25, or 100 μM IPTG (isopropyl β-D-thiogalactopyranoside) and 0.1% deoxycholate. Plates were incubated for 18 h at 30 °C and photographed after being kept at 4 °C overnight.

Cell Division Phenotypes of *damX* SPOR Mutants in a *damX dedD* Double-Mutant Background. IPTG-inducible *gfp-damX* fusions (either wild-type or *damX* mutants) were integrated into the chromosome of EC1926 (*dedD damX*<>-

kan) in a single copy at the Φ80 attachment site using spectinomycin-resistant CRIM vectors as described previously.[4,29] Strains were grown overnight at 30 °C in LB medium containing 25 μg/mL spectinomycin. In the morning, cultures were diluted 1:500 in LB without antibiotic but containing 0−2 mM IPTG. These cultures were grown for ∼4 h at 30 °C to an OD$_{600}$ of 0.5, at which point samples were taken for Western blotting, phase contrast microscopy, and fluorescence (GFP) microscopy. A subset of mutant proteins was also tested without the GFP tag. For these experiments, *damX* variants were cloned into pDSW204, which allows for the IPTG-inducible expression of genes under control of a modified Trc promoter. Plasmids were transformed in EC1926. Transformants were grown and analyzed as for the chromosomal integrants, except that the medium always contained 200 μg/mL ampicillin to maintain plasmids and cells were not photographed via fluorescence microscopy.

■ RESULTS

Structure Determination. DamX is a bitopic membrane protein with a C-terminal SPOR domain (Figure 1A). To determine the structure of the SPOR domain, we cloned residues 338−428 into an expression vector that provided an

N-terminal His$_6$ purification tag. The isotopically labeled His$_6$-SPOR domain was overproduced in *E. coli* and purified by cobalt affinity chromatography. The purified protein was soluble at up to 80 mg/mL and bound PG.[4] Backbone resonances were assigned using the standard technique of a backbone walk with no difficulties. An assigned ^{1}H−^{15}N HSQC spectrum is shown in Figure 2. Aside from His$_6$ tag resonances, which could not be unambiguously assigned, the only unassigned amide resonance corresponds to asparagine 381, which lies in the short loop between the second and third β-strands. Given the high quality of the data, one can only speculate that this resonance is 100% degenerate with another amide.

Complete but nonstereospecific side chain assignments (Table S4 of the Supporting Information) were made mostly from H(CCO)NH-, C(CO)NH-, and HCCH-TOCSY experiments. An initial set of NOEs was identified for which both protons could be unambiguously assigned and used to calculate an initial family of structures. This initial fold was used to assign further NOEs unambiguously, and the list of distance restraints was further refined during subsequent rounds of structure calculations in an iterative manner. The final ensemble of structures for the DamX SPOR domain was generated by taking the 25 lowest-energy structures from an ensemble of 250 calculated structures. None of the structures had any experimental restraint violations in excess of 0.5 Å (NOEs), 5° (dihedral angles), or 2 Hz (RDCs). All statistics and discussion will focus on the actual SPOR domain (residues 344−428 in DamX); a summary of structural statistics can be found in Table 1. In all figures, the first 21 residues of the construct have been omitted because they are essentially unstructured (data not shown). The omitted amino acids comprise 10 from the His$_6$ tag, 5 from a synthetic linker, and 6 DamX-derived residues that presumably precede the start of the SPOR domain per se.

Figure 1C shows a backbone trace (Cα, CO, and N) through all 25 members of the final ensemble and a ribbon representation of the molecule in both side-on and bottom-up orientations. The backbone rmsd for this ensemble is 0.795 Å but improves to 0.663 Å if the final α-helix (starting at residue 420) is excluded; this helix is the least well-defined part of the SPOR domain. The structure also has good Ramachandran characteristics: as determined by PRO-CHECK-NMR,[46] 98.3% of residues fall in the most favorable (70.4%) and allowed regions (27.9%). None of the amino acids analyzed (glycines and prolines are excluded) for the ensemble of 25 structures have ϕ and ψ angles that fall in the disallowed region of Ramachandran space.

The DamX SPOR Domain Belongs to the RNP Fold Family. In terms of secondary structure, the domain contains four β-strands and three α-helices, which are arranged in a βαββαβα topology. The four β-strands comprise a concave antiparallel β-sheet on one face of the molecule, arbitrarily shown as the bottom face in Figure 1C. Helices α1 and α2 pack along the top of the β-sheet; α2 is discontinuous because of the presence of a proline residue (P407). The C-terminal helix, α3, is short and packs against the bottom of the β-sheet, partially occluding this face of the molecule.

Overall, the structure of DamX's SPOR domain looks like an RNP domain, a very common fold characterized by two α-helices flanking a single four-stranded β-sheet. RNP stands for ribonucleoprotein and refers to the fact that the first examples of this fold were RNA binding domains.[19] This fold has since

Table 1. Structural Statistics for the Final Ensemble of DamX (25 structures)^a

no. of experimental restraints	
short-range NOEs ($|i − j| \leq 1$)	898
medium-range NOEs ($1 < |i − j| < 5$)	253
long-range NOEs ($|i − j| \geq 5$)	450
total unambiguous NOEs	1601
NOEs with multiple assignments	361
total NOEs	1962
distance restraints per residue	23.3
φ and ψ angles	162
backbone amide RDCs	62
no. of restraint violations	
NOE distances violated >0.5 Å	0
dihedral angles violated >5°	0
RDCs violated >2 Hz	0
rmsds from experimental restraints	
NOE (Å)	0.0123 ± 0.0016
dihedrals (deg)	0.139 ± 0.040
RDCs (Hz)	0.149 ± 0.037
average overall XPLOR energy (kcal/mol)	139.61 ± 4.14
rmsd from idealized geometry	
bond lengths (Å)	0.0022 ± 0.0001
bond angles (deg)	0.423 ± 0.005
impropers (deg)	0.243 ± 0.004
structure Z scores	
Ramachandran plot quality	−3.4
first-generation packing quality	−1.6
second-generation packing quality	3.3
χ_1/χ_2 rotamer normality	−4.9
backbone conformation	−1.7
Ramachandran plot statistics (%)	
most favored regions	70.4
additionally allowed regions	27.9
generously allowed regions	1.7
disallowed regions	0.0
coordinate rmsd (residues 344−428, average difference from the mean, Å)	
backbone atoms	0.795
heavy atoms	1.296

^{a}All statistics are for the actual SPOR domain (residues 344−428) in all 25 structures, except restraint violations, rmsds, and energies are for all 106 residues in the construct. Structural statistics are taken from the output of XPLOR-NIH[40,41] with the exception of the Ramachandran statistics, which come from PROCHECK-NMR.[46] The Ramachandran plot quality value is from the PSVS server (http://psvs-1_4-dev.nesg.org/); the remaining Z scores were generated using the iCING server (http://nmr.cmbi.ru.nl/cing/iCing.html).

been found in many proteins and is no longer considered to be associated with a particular class of ligand. Yang et al.[16] noted that the SPOR domain from FtsN adopts an RNP fold. A DALI search using the lowest-energy structure for DamX's SPOR domain returned many statistically significant matches, including the SPOR domain from CwlC (Z = 3.6; rsmd = 3.7 Å; PDB entry 1x60-A), a PII-like domain from SA1388, a *Staphylococcus aureus* protein of unknown function (Z = 3.4; rmsd = 6.8 Å; PDB entry 2nyd-B), and more than a dozen eukaryotic RNA-binding proteins, such as Splicing Factor 45 (Z = 3.3; rmsd = 3.8 Å; PDB entry 2peh-A). Interestingly, the SPOR domain from FtsN was not among the statistically significant matches.

Backbone Dynamics. Measured NMR relaxation parameters were analyzed according to the model free formalism[36,37] using Fast-Modelfree and ModelFree version 4.20.[34,38,39] Regions of the domain with high mobility are illustrated in Figure 3. An overall rotational correlation time, τ_m, of 6.98 ns
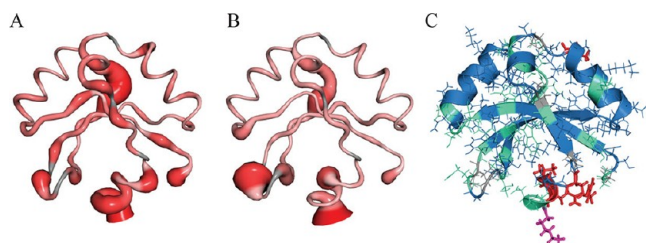

Figure 3. NMR relaxation dynamics of the DamX SPOR domain. (A and B) Sausage figures depicting $^{15}N-\{^1H\}$ NOE and S^2 values, respectively. Increasing flexibility (smaller values) is indicated by both increasing width and a deeper red color. (C) Structure colored according to motional models as determined by ModelFree version 4.20: blue for model 1 (S^2, with global tumbling only), green for model 2 (S^2 and fast internal motions), red for model 4 [S^2, fast internal motion, and chemical exchange (R_{ex})], and magenta for model 5 (S^2 and both fast and slow internal motions). No residues are best described by model 3.

suggests that the DamX SPOR domain tumbles in solution as a well-structured monomer. However, several areas of increased flexibility are indicated by reduced values for both order parameters (S^2) and $\{^1H\}-^{15}N$ NOE values. One is the $\alpha1-\beta2$ loop at the top rear of the structure as depicted in Figure 3. Two other regions exhibiting increased levels of motion are the $\beta2-\beta3$ loop at the lower left as well as $\alpha3$ through the C-terminus at the bottom center of the figure.

In addition to the general flexibility described by the order parameters and NOE values, the ModelFree formalism attempts to categorize the motions of each residue into various models based on their time scales. The majority of residues in the DamX SPOR domain fit into model 1 (global tumbling only, S^2) or model 2 (S^2 and fast internal motion). No amino acids in this protein are well fit by model 3 (S^2 and chemical exchange, R_{ex}). Several residues are more dynamic; T405, R421, V423, and Q424 are best described by model 4 (S^2, fast internal motion, and R_{ex}), and K428 is best described by model 5 (S^2 and both fast and slower internal motions). The chemical exchange of T405 may simply arise from it being located near the proline kink that breaks up helix 2. The chemical exchange of R421, V423, and Q424, as well as the more complex motions of K428 at the C-terminus, is consistent with enhanced overall motion of $\alpha3$.

Identification of Three Amino Acids Important for Septal Localization. We targeted nine amino acids for mutagenesis (Figures 1B and 4). Two of these, Gln 351 and Ser 354, were targeted because they are the most highly conserved surface-exposed residues as revealed by an alignment of 132 SPOR domains that was mapped onto the surface of the SPOR domains of CwlC and DamX using Consurf (Figure S1 of the Supporting Information).[47] Four amino acids were targeted because they correspond to residues suggested by Mishima et al.[15] to interact with PG in CwlC: Asn 357, Asn 360, Ser 395, and Glu 398. Finally, three tryptophans (residues 364, 385, and 416) were targeted because their side chains exhibited a modest NMR chemical shift when the DamX SPOR domain was incubated with muropeptides derived by digesting *B. subtilis* PG
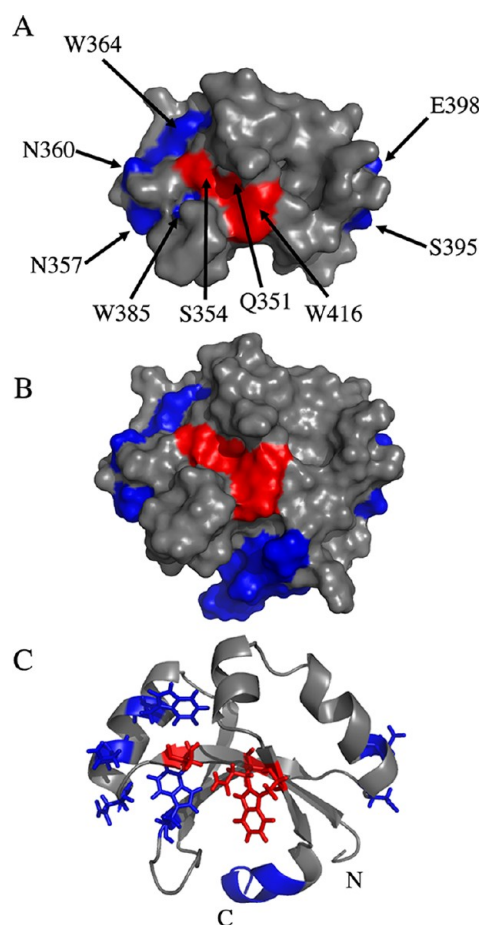

Figure 4. Amino acids targeted for mutagenesis. Residues found to be important for septal localization are colored red, while residues found to be unimportant are colored blue. (A) Space-filling model of the SPOR domain from DamX with the final helix, $\alpha3$, omitted for the sake of clarity. (B) Same as panel A but with $\alpha3$. (C) Ribbon diagram of the SPOR domain with targeted residues illustrated as stick models, except for the portion of $\alpha3$ that was deleted.

to completion with mutanolysin (Figure S2 of the Supporting Information). (Whether muropeptides are physiologically relevant ligands is not known. We used muropeptides from *B. subtilis* rather than *E. coli* because they were already on hand from an unrelated experiment, the two organisms have a very similar muropeptide profile, and a *B. subtilis* SPOR domain has been shown to localize to the midcell when produced in *E. coli*.[5,48−50])

The mutant SPOR domains were fused to Tat-targeted GFP (^{TT}GFP) to direct their export to the periplasm via the Tat system and produced from plasmids in a wild-type *E. coli* background. Septal localization was assayed by fluorescence microscopy of live cells. The results are summarized in Figure 5A and Table S5 of the Supporting Information (including exposure times, which varied because some fusion proteins were brighter than others). The wild-type ^{TT}GFP-DamX SPOR domain fusion protein appeared as a bright band of fluorescence at the midcell in ∼80% of the cells, similar to our previous report.[4] Comparable frequencies of septal localization were observed for proteins with substitutions at Asn 357, Asn 360, Ser 395, or Glu 398. These lesions should have impaired the previously proposed PG binding sites near the start of $\alpha1$ and $\alpha2$.[15] Even a double-mutant protein
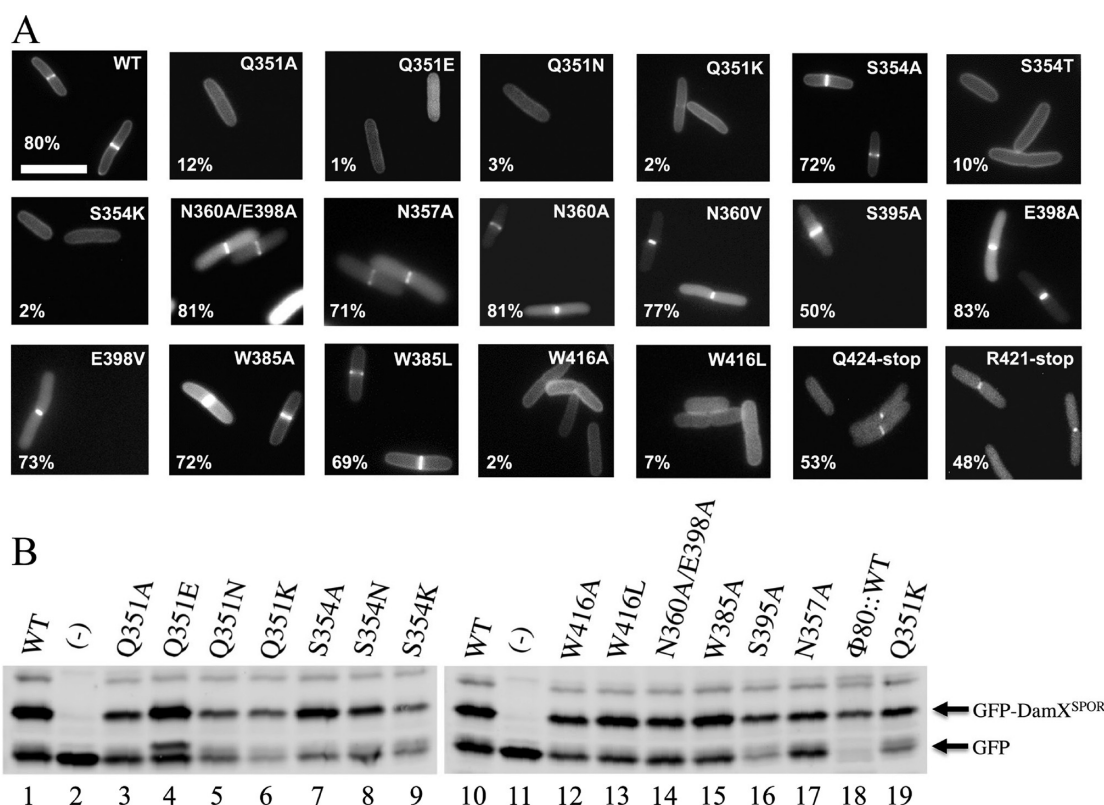
Figure 5. (A) Septal localization activities of several mutant SPOR domains. The images are fluorescence micrographs of live cells producing ^{TT}GFP-DamX^{SPOR} proteins, either wild type (WT) or with the indicated amino acid substitution or deletion. Numbers at the bottom left of each image are the percentages of cells in the population scored as having septal localization. The scale bar is 5 μm. (B) Western blot showing the abundance of several ^{TT}GFP-DamX^{SPOR} proteins, as indicated [($-$) is a ^{TT}GFP vector control]. Proteins shown on both blots come from independent samples and illustrate day-to-day variation (e.g., Q351K).

(N360A/E398A) with substitutions in both proposed sites localized as efficiently as the wild type. Essentially wild-type localization was also observed when Trp 385 was changed to either Ala or Leu. Multiple substitutions at Trp 364, whose side chain is buried in the domain, resulted in the production of nonfluorescent GFP fusion proteins (not shown), so we assume this residue is important for folding.

Substitutions at Q351, S354, or W416 (all of which are in the β-sheet) generally reduced the level of septal localization to <10% of the cells in the population. The poorly localizing proteins often appeared as fluorescent halos illuminating the outline of the cells, suggesting the proteins either diffuse freely in the periplasm or associate with PG in a relatively nonspecific manner. An interesting exception was the S354A mutant protein, which localized about as well as the wild type. This finding is consistent with SPOR domain alignments showing that Ser and Ala occur with roughly equal frequency at this position (Figure 1B and Figure S1 of the Supporting Information). Apparently, the size of the residue at position 354 is important but the hydroxyl moiety is not.

Evaluating Expression and Folding of the Non-localizing SPOR Domain Mutants. Western blotting revealed that the mutant ^{TT}GFP-DamX^{SPOR} proteins were not all produced at the same level (Figure 5B), consistent with the variations in photographic exposure times needed to visualize the various proteins in vivo (Table S5 of the Supporting Information). The different expression levels raised two related concerns about the interpretation of the localization experiments. One is whether low abundance per se prevents

detection of septal localization. The other is whether the mutant proteins have folding or stability defects that render the localization phenotypes meaningless.

With regard to the impact of ^{TT}GFP-DamX^{SPOR} abundance on scoring of septal localization, the fact that we could detect low-abundance mutants like Q351K as fluorescent halos argues we would have seen a band at the midcell had there been one. Moreover, some of the mutant proteins that localized poorly were produced at levels similar to that of the wild type (e.g., Q351E and W416L in lanes 4 and 13, respectively, of Figure 5B). Conversely, some mutant proteins localized well despite being of low abundance (e.g., compare the localizers S395A and N357A to the nonlocalizer Q351K in lanes 16–19 of Figure 5B). Finally, to make a direct assessment of how ^{TT}GFP-DamX^{SPOR} abundance affects scoring of septal localization, we lowered production of the wild-type construct by integrating it into the chromosome in a single copy at the Φ80 attachment site. When this strain was grown without IPTG, levels of the GFP fusion protein were as low as those of any of the localization-defective mutants (Figure 5B, lane 18). Nevertheless, we detected septal localization in ~55% of the cells, and increasing levels of expression via induction with IPTG had a more profound effect on the brightness of the septal bands than on their frequency (Figure S3 of the Supporting Information).

We also verified that the localization-defective mutant proteins were for the most part well folded by purifying them and collecting HSQC spectra. The spectra for the Q351A, Q351E, Q351N, S354T, and W416A proteins were very similar to that of the wild type (Figure S4 of the Supporting
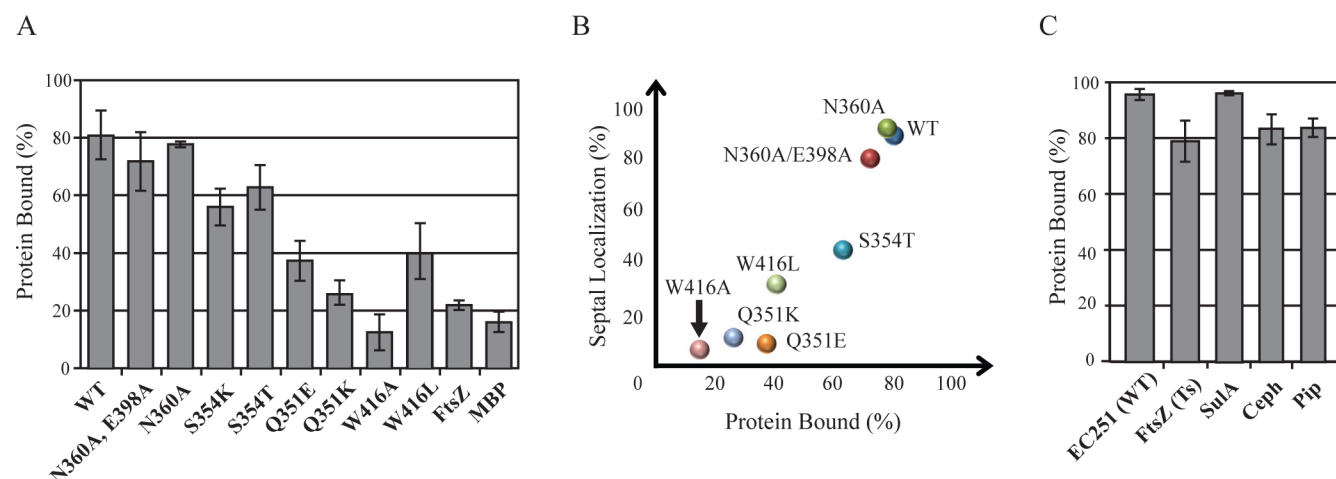
Figure 6. Peptidoglycan binding assay. (A) PG binding activities of SPOR domains with the indicated amino acid substitutions as determined by the fraction of input protein that cosedimented with isolated PG sacculi upon ultracentrifugation at 4 °C. Bars indicate the average and standard deviation from at least three experiments. FtsZ and MBP (maltose binding protein) were assayed as negative controls. (B) Scatter plot showing the correlation of septal localization assayed in live cells grown at 21 °C with PG binding activity data from panel A. (C) Binding of the wild-type SPOR domain to different PG preparations. EC251(WT) refers to sacculi from wild-type cells harvested in the exponential growth phase. FtsZ(Ts) and SulA refer to sacculi from filamentous cells in which division was blocked by interfering with FtsZ function. Ceph and Pip refer to sacculi from filamentous cells in which division was blocked by interfering with FtsI function using the β-lactam cephalexin or piperacillin.

Information). However, the HSQC spectrum of the Q351K mutant revealed some extra peaks, suggesting this protein interconverts between two or more conformations and is not as close to the native structure as the other mutants (Figure S4C of the Supporting Information).

The C-Terminal α-Helix Is Dispensable for SPOR Domain Localization. The data presented so far argue the β-sheet of DamX is important for septal localization. The simplest interpretation is that the β-sheet binds septal PG, but a short C-terminal α-helix designated α3 appears to limit access to the β-sheet (Figure 1C). SPOR domain alignments indicate α3 is conserved in DamX proteins but absent from CwlC and FtsN, suggesting it has an important function special to DamX (Figure 1B). We therefore constructed TTGFP fusions with two derivatives of the SPOR domain in which α3 was removed via truncation at R421 and Q424. Our prediction was that removing α3 would increase the levels of both septal localization and PG binding, but technical issues prevented us from making much headway with these issues. Cells producing TTGPF-DamXSPOR α3 deletion mutants were dim, and Western blotting revealed the mutant proteins were produced at approximately one-third the level of the wild type (Figure S5 of the Supporting Information). Nevertheless, both truncated proteins localized to the septal ring in 50% of the cells in the population (Figure 5A and Table S5 of the Supporting Information). We purified the R421 deletion protein with the intent of assaying it for binding to PG, but HSQC spectra of the ¹⁵N-labeled protein revealed spectral collapse, indicative of loss of secondary structure (Figure 4G of the Supporting Information). With regard to the apparent contradiction that the truncated protein localizes relatively well despite having a serious folding or stability defect, it must be noted that NMR is conducted using the SPOR domain that has been out of the cell for at least 2 days.

PG Binding Assays. If septal localization is driven by binding of SPOR domains to septal PG, then the localization-defective mutants should bind poorly. Unfortunately, isolated septal PG is not available, and the features of PG recognized by

SPOR domains have yet to be defined. As a surrogate ligand, we used PG sacculi isolated from *E. coli* cells in exponential growth; sacculi from such cultures are predicted to contain septal PG because many of the cells are dividing at the time of harvest (but see below). In the binding assay, a mixture of SPOR domain protein and PG sacculi is subjected to centrifugation, which causes the sacculi to sediment. Samples of the pellet and supernatant are then analyzed by sodium dodecyl sulfate−polyacrylamide gel electrophoresis to determine how much SPOR domain protein is in each fraction. As a control, SPOR domains are also centrifuged in the absence of sacculi to verify that they do not simply sediment on their own. Previously, we reported that ∼80% of the DamX SPOR domain cosedimented with PG, as compared to only ∼20% of two negative control proteins, the cytoplasmic GTPase FtsZ and the periplasmic maltose transport protein MBP.[4]

We tested six localization-defective DamX SPOR mutants in the cosedimentation assay: Q351E, Q351K, S354T, S354K, W416A, and W416L. We also tested the wild type and two mutants that localized well, N360A and the N360A/E398A double mutant, which were chosen because they have lesions in the previously proposed PG binding sites in CwlC.[15]

The results of the binding assay were for the most part consistent with expectations (Figure 6A). The wild type and the two localization-proficient mutant proteins bound PG well, whereas four of the localization-defective mutant proteins did not. However, two mutant proteins behaved anomalously: S354T and S354K bound PG almost as well as the wild type despite exhibiting a profound localization defect. In thinking about potential explanations for the discrepancy, we realized binding was assayed at 4 °C but localization was assayed using cells grown at 30 °C. The subset of TTGFP-DamXSPOR constructs used in the PG binding assay was therefore tested for localization in cells grown at 21 °C. The S354K mutant protein was too dark to visualize, presumably because of a folding defect at the lower temperature, and had to be excluded from the analysis. All of the other proteins localized better at 21 °C. In most cases, the improvement was small, but the S354T mutant protein localized much better. When the localization

Table 2. Characterization of DamX SPOR Domain Mutants (fused to GFP)

Map of GFP-DamX constructs[a]		ΔdamX background[b]		ΔdamXdedD background[e]	
		Septal Localization (%)[c]	DC resistance[d]	Rescue division[f]	Inhibit division[f]
	GFP-DamX(WT)	71 ± 4	+++	+++	+++
	GFP	0	-	-	-
	GFP-DamX(Q351K)	8 ± 1	-	-	-
	GFP-DamX(S354K)	26 ± 6	+/-	-	-
	GFP-DamX(W416L)	40 ± 7	+	-	-
	GFP-DamX(Δ350-428)	2 ± 1	-	-	-
	GFP-DamX(Δ346-428)	2 ± 1	-	-	-

[a]For the sake of clarity, domains are not drawn to scale. Abbreviations: Cyto, cytoplasmic domain; TM, transmembrane helix; Linker, putative unstructured linker region; SPOR, SPOR domain. [b]The following derivatives of EC1910 were used: EC2882, EC2884, EC2886, EC2888, EC2965, EC2966, and EC2967. [c]The percentage of cells in the population judged to have a fluorescent band at the division site. Values are the average ± the standard deviation of two to six separate assays, with at least 100 cells scored each time. [d]Growth in the presence of 0.1% deoxycholate. See Figure S7 of the Supporting Information for the original data. [e]The following derivatives of EC1926 were used: EC2312, EC2313, EC2314, EC2315, EC2316, EC2785, and EC2786. [f]Cell length during growth in the presence of various concentrations of IPTG. See Figure S8 of the Supporting Information for the data.

data from 21 °C are used as the basis of comparison, there is a good correlation between localization and PG binding (Figure 6B).

We also investigated whether the pull-down assay faithfully reflects binding to septal PG, as reported previously for the periplasmic domain of FtsN.[9] We isolated sacculi from filamentous cells obtained after blocking cell division in four ways: shifting an *ftsZ*(Ts) mutant to 42 °C, inducing the FtsZ inhibitor *sulA*, or inactivating the septal PG synthase FtsI with cephalexin or piperacillin. In all cases, the average cell length was >20 μm at the time of harvest. When the amount of PG from the various preparations was normalized according to *N*-acetylglucosamine content, the SPOR domain from DamX bound as well to "filamentous" sacculi as to sacculi from a culture that was dividing normally (Figure 6C). This result is clearly different from what was reported for FtsN and might mean that, at least for the SPOR domain from DamX, the cosedimentation assay measures a general affinity of PG rather than site-specific binding (see Discussion).

The SPOR Domain Is Required for the Proper Function of *damX* in a Variety of Biological Assays. The experiments described so far were conducted with isolated SPOR domains, but we were also interested in whether DamX's SPOR domain has much relevance for DamX function in vivo. This question may seem like a straw man, but three studies have addressed this issue in the case of FtsN, which unlike DamX is essential for cell division.[51] All three studies concluded that the SPOR domain makes little or no contribution to the ability of FtsN to support cell division, although the two studies that looked specifically at septal localization agreed the SPOR domain is very important for this activity.[5,6,9]

We constructed a set of IPTG-inducible *gfp-damX* fusions with deleterious amino acid substitutions in the SPOR domain: Q351K, S354K, or W416L. We also constructed two SPOR domain deletion mutants, which were truncated after S345 and T349. These residues are two and five amino acids into the SPOR domain, respectively, according to the alignment shown in Figure 1B. As a positive control, we used a *gfp* fusion to full-length wild-type *damX*, and as a negative control, we used *gfp* alone. The *gfp* fusion constructs were integrated into the chromosome at the Φ80 attachment site using CRIM vector

technology.[29] To assess septal localization and deoxycholate sensitivity, we integrated the constructs into a *damX* null mutant. To assess the ability of these constructs to promote and inhibit cell division, we integrated them into a *damX dedD* double mutant. The double-mutant background was employed because a simple *damX* null is not filamentous, but combining a *damX* null mutation with a *dedD* null mutation exacerbates the mild filamentation and chaining defect caused by deleting *dedD*.[4,5]

First, we assayed production of the various fusions by Western blotting. When the wild-type *gfp-damX* fusion was induced with 10 μM IPTG, the amount of GFP-DamX in the cells was comparable to the amount of DamX normally present in *E. coli* grown under the same conditions (Figure S6A of the Supporting Information). Inducing with 100 μM IPTG resulted in 4−8-fold overproduction, depending on the day (Figure S6A of the Supporting Information). Finally, the wild-type GFP-DamX fusion was consistently approximately twice as abundant as the mutant fusion proteins when assayed in a *damX* mutant background, but these proteins were all produced at similar levels in the *damX dedD* double-mutant background (Figure S6B,C of the Supporting Information). Thus, the Q351K and S354K substitutions had little or no effect on the expression of full-length *gfp-damX* fusions even though they significantly reduced the abundance of the corresponding [TT]GFP-DamX SPOR constructs.

We then tested the relevance of the SPOR domain for DamX function in a *damX* mutant background. Deletion of the SPOR domain from DamX essentially eliminated septal localization, as did the Q351K substitution (Table 2). Interestingly, the S354K and W416L substitutions also impaired localization, but these lesions were not nearly as deleterious in the context of full-length DamX as in the context of the isolated SPOR domain. Results from the deoxycholate sensitivity test paralleled the localization results. Thus, the SPOR domain deletion constructs and the Q351K mutant protein did not confer any resistance, whereas the S354K and W416L mutant proteins conferred some resistance if they were overproduced (Table 2 and Figure S7 of the Supporting Information).

Next, we examined the ability of the *gfp-damX* constructs to improve or inhibit cell division in a *damX dedD* background.

This proved to be much more difficult than we had anticipated. Two previous studies, including one from our lab, reported the double mutant had an average length of ~15 ± 13 μm, while the *dedD* single mutant had a length of ~6 ± 8 μm.[4,5] These means are sufficiently different that determining whether introduction of a *gfp-damX* fusion reverts the double mutant to the phenotype of the single mutant seemed like it should be straightforward, but the relatively large standard deviations indicate a problem: populations of these mutants consist of many cells that are only slightly elongated and occasional cells that are much longer than normal. This makes estimates of the mean length very sensitive to sampling procedures. In this study, we were more careful to sample (photograph) cells at random and we report geometric means, which are better measures of central tendency than arithmetic means when lengths do not follow a normal distribution. Finally, we tested the effect of *gfp-damX* fusions at multiple IPTG concentrations because for the wild-type construct low levels rescue division but high levels inhibit division. Our findings are summarized in Table 2 and presented in more detail in Figures S8 and S9 of the Supporting Information.

The *damX dedD* double mutant had a length of ~11 μm, which decreased to ~8 μm when *gfp-damX* was induced with 10 μM IPTG and increased to ~20 μm at 100 μM IPTG. None of the *gfp-damX* SPOR domain mutant constructs convincingly rescued or inhibited division at IPTG concentrations ranging from 10 μM to 2 mM, although close inspection of Figure S8 of the Supporting Information suggests that perhaps S354K rescued division slightly at high IPTG concentrations while W416L rescued division slightly at moderate IPTG concentrations but then started to inhibit division as the IPTG concentration was increased. Localization of the GFP-DamX SPOR domain constructs in the *damX dedD* double mutant paralleled results obtained for the *damX* single mutant. To wit, both deletion constructs and the Q351K protein exhibited little or no localization to potential division sites, the S354K protein localized sporadically, and the W416L protein localized moderately well (Figure S9 of the Supporting Information).

To address the possibility that the complementation defect was an artifact of including a GFP tag in our constructs, we verified that DamX(Q351K) and DamXΔ(349−428) mutant proteins failed to rescue division when produced from plasmids without the tag (Figure S10 of the Supporting Information). We also verified expression of these constructs by Western blotting with the anti-DamX antibody (Figure S10 of the Supporting Information).

■ DISCUSSION

Comparison of SPOR Domains from DamX, CwlC, and FtsN. Figure 7 compares the solution structures reported for the SPOR domains of DamX, CwlC, and FtsN. Note that all three SPOR domains adopt a similar fold despite sharing less than 20% amino acid identity in pairwise comparisons (Figure 1B). This fold is known as an RNP (ribonucleoprotein) fold, also called an RBD (ribonucleotide binding domain) or RRM (RNA recognition motif). The fold was originally identified as a single-stranded RNA binding motif, but some members of this structural superfamily bind to protein, DNA, and, in the case of the SPOR domains, PG. RNP domains are characterized by a βαββαβ secondary structure wherein the four β-strands comprise an antiparallel β-sheet buttressed on one side by the two α-helices.
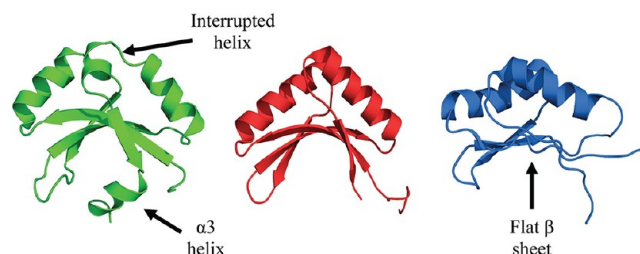

Figure 7. Comparison of the solution structures of the SPOR domains from DamX (green, this study), CwlC (red, PDB entry 1x60), and FtsN (blue, PDB entry 1UTA). Structures were rendered using PyMOL.[42]

Despite the overall similarity among the three SPOR domain structures, there are a few noteworthy differences. First, in DamX α2 is interrupted by a proline, resulting in a sharp kink in that feature. While the proline is conserved in all DamX sequences, it is not present in CwlC or FtsN; therefore, α2 is longer in those proteins, and the loop connecting α2 with β4 is longer as well. Whether the kink has any biological relevance is not known. Second, DamX and CwlC have a concave β-sheet that forms a cleft, whereas the β-sheet of FtsN is rather flat. These differences are intriguing because our working hypothesis is that the β-sheet is the PG binding site. If this is true, we would expect the β-sheet has to adopt a very similar overall conformation in all three domains when they are bound to PG. Perhaps the different conformations represent "closed" and "open" states sampled by all three domains. The third major difference is the extra helix, designated α3, located at the C-terminus of DamX. This difference is also interesting because, assuming PG binds to the β-sheet, α3 might have to move out of the way and could regulate binding.

The β-Sheet Is Important for Septal Localization and Possibly for PG Binding. The β-sheet is the primary ligand binding surface in many members of the RNP fold superfamily.[17,19−22,52,53] Consistent with this theme, we found that mutations at Q351, S354, and W416—all of which are in the β-sheet and have solvent-exposed side chains—impair septal localization and PG binding (Figures 5 and 6). Moreover, Q351 and S354 correspond to the most highly conserved surface-exposed residues in SPOR domains (Figure S1 of the Supporting Information), but the binding results must be considered tentative because our assay used PG sacculi rather than isolated "septal PG", by which we mean the still undefined form of PG to which SPOR domains are thought to bind.

Until now, it has been thought that the cosedimentation assay using purified PG sacculi reflected specific binding of the SPOR domain to septal PG. This inference stems from an earlier report showing the periplasmic domain from FtsN bound better to sacculi from dividing cells than to sacculi from cells that were not dividing.[9] We performed an analogous experiment using the SPOR domain from DamX but observed equivalent binding when input PG was matched by N-acetylglucosamine content (Figure 6C). We do not know whether the discrepancy between the two reports reflects a real difference between the proteins assayed or a technical problem. It is worth noting, however, that the experimental design requires accurately matching the amount of PG used in each trial, which is challenging because PG is insoluble and difficult to aliquot reproducibly. Regardless of the origin of the discrepancy, it is clearly a high priority to develop better

binding assays that use chemically defined, physiologically relevant PG fragments.

The indifference of DamX's SPOR domain to whether the sacculi were obtained from dividing or filamentous cells raises questions about the species to which the SPOR domain is actually binding in the cosedimentation assay. One possibility is that septal PG is lost from the sacculi during the purification procedure, which involves harsh processes like boiling in SDS. If septal PG is lost, then the assay might reflect a general propensity of SPOR domains to bind bulk PG. Nonlocalizing mutant proteins might bind poorly because the β-sheet is used for both site-specific and nonspecific binding to PG. This idea is analogous to that for many site-specific DNA binding proteins, which typically have a general affinity for DNA and a higher affinity for a specific DNA site. Another possibility is that the SPOR domain is binding septal PG in the cosedimentation assay, but this structure is not unique to the septum. For example, amidases probably contribute to PG turnover during elongation, so glycan strands that lack stem peptides could be found in both the septum and the cell cylinder. If these glycan strands are not firmly anchored to the sacculus, the ones that remain after sacculi have been purified might be relatively uniformly distributed. We considered the possibility that SPOR domains might be excluded from the cell cylinder by Lpp and thus accumulate at the midcell where there is a large amount of new PG that has yet to acquire Lpp. Because one of the steps in the procedure used to purify sacculi involves treatment with a protease to remove Lpp, the purification process might alter the distribution of SPOR domain binding sites. However, this does not appear to be a viable hypothesis because SPOR domains localize sharply to the midcell in an Lpp null mutant (A. Yahashiri and D. Weiss, unpublished observations).

An unexpected finding was that amino acid substitutions at Q351, S354, and W416 had a more dramatic effect on septal localization of isolated SPOR domains than on septal localization of full-length DamX proteins. We can envision several potential explanations for this discrepancy. First, parts of DamX outside of the SPOR domain might interact with other septal ring proteins and thus contribute directly to septal localization. In support of this idea, DamX interacts with several septal ring proteins in a bacterial two-hybrid system,[4] but we did not detect septal localization of DamX when the SPOR domain was deleted; therefore, any targeting domains other than the SPOR domain would have to be rather weak. Second, whereas ^{TT}GFP-DamX^{SPOR} proteins are free to diffuse throughout the periplasm, in the context of the complete DamX protein the SPOR domain is tethered to the inner membrane and may thus be maintained in relatively high local concentrations with respect to the PG layer. Finally, NMR and dynamic light scattering indicate the isolated DamX SPOR domain is monomeric (not shown), but DamX interacts with itself in a bacterial two-hybrid system, suggesting the full-length protein is a dimer, which could have a much higher affinity for PG and might better tolerate mutations that reduce affinity.

α3 Is Not Required for Septal Localization, but the Question of Whether It Regulates Localization Needs Further Study.

If the β-sheet of the SPOR domain binds PG, or any other ligand for that matter, α3 probably has to move out of the way. Consistent with this possibility, NMR relaxation data revealed α3 is one of the most dynamic parts of the DamX SPOR domain. We therefore predicted that removing α3 would improve both septal localization and binding to PG. Unfortunately, the deletion proteins we constructed to test

this notion were not very stable, so the only solid conclusion that can be drawn at this time is that α3 is not required for septal localization. Efforts to circumvent the folding issues by substituting individual amino acids in α3 also resulted in unstable proteins (A. Yahashiri and D. Weiss, unpublished observations). We therefore doubt that genetic approaches have much potential to resolve the question of whether α3 moves to allow ligand binding. It will probably be more fruitful to determine the structure of the SPOR domain in complex with a PG fragment.

DamX Requires an Intact SPOR Domain for Proper Function in Vivo.

The fact that so many bacterial proteins contain SPOR domains argues for their importance. Here we showed that DamX requires an intact SPOR domain to localize to the septal ring, similar to previous reports for FtsN.[5,9] Thus, the SPOR domain of DamX is not only sufficient for septal localization[4,5] but also necessary, and there are no other potent septal targeting domains in the protein. Although FtsN proteins that lack the SPOR domain still support reasonably efficient cell division,[5,6,9] this is not true of DamX, which requires an intact SPOR domain for every activity we assayed: to correct the division defect of a *damX dedD* double mutant, to confer full resistance to deoxycholate, and to inhibit cell division when DamX is overproduced. Even the W416L mutant protein was defective in these functions despite the fact that this lesion impaired septal localization only modestly. Our finding that DamX must have an intact SPOR domain to inhibit division complements previous reports that overproduction of isolated SPOR domains impairs division.[4,5] Perhaps too much SPOR domain displaces FtsN or blocks the access of other proteins to septal PG. It will be interesting to explore whether the SPOR domain from DamX can be functionally replaced with SPOR domains from unrelated proteins, as this experiment should give some insight into whether the SPOR domain is important only because it delivers DamX to the septal ring or whether it has a more sophisticated function.

■ ASSOCIATED CONTENT

Ⓢ Supporting Information

A description of strain and plasmid construction, a strain table, a plasmid table, a primer table, a table of assigned chemical shifts, a table quantifying localization of mutant SPOR domains, a plot of surface conservation on the SPOR domains from CwlC and DamX, an alignment of 132 SPOR domains, a plot of chemical shifts induced by incubating PG fragments with the DamX SPOR domain, a figure documenting the effect of ^{TT}GFP-DamX SPOR abundance on scoring of septal localization, comparisons of the HSQC spectra of wild-type and mutant DamX SPOR domains, a Western blot documenting expression of DamX SPOR domains with deletions of α3, Western blots documenting expression of *gfp-damX* fusions used in this study, photographs of plates used to score growth in the presence of deoxycholate, a bar graph depicting the effect of GFP-DamX proteins on cell division, phase contrast and fluorescence images documenting localization and division phenotypes associated with these GFP-DamX proteins, and a figure documenting the effect of DamX proteins (without a GFP tag) on cell division. This material is available free of charge via the Internet at http://pubs.acs.org.

■ AUTHOR INFORMATION

Corresponding Author

*C.A.F. for NMR: telephone, (319) 384-2937; fax, (319) 335-7273; e-mail, andrew-fowler@uiowa.edu. D.S.W. for molecular biology: telephone, (319) 335-7785; fax, (319) 335-9006; e-mail, david-weiss@uiowa.edu.

Present Address

∥Vertex Pharmaceuticals, Inc., 2500 Crosspark Rd., E200, Coralville, IA 52241.

Author Contributions

K.B.W. and A.Y. contributed equally to this work.

Notes

The authors declare no competing financial interest.

■ ABBREVIATIONS

PG, peptidoglycan; RNP, ribonucleoprotein; ^{TT}GFP, Tat-targeted green fluorescent protein; CRIM plasmids, conditional-replication, integration, and modular plasmids; Δ, deletion; NOE, nuclear Overhauser effect; NOESY, NOE spectroscopy; TOCSY, total correlation spectroscopy; HSQC, heteronuclear single-quantum correlation spectroscopy; rmsd, root-mean-square deviation.

■ REFERENCES

(1) de Boer, P. A. (2010) Advances in understanding *E. coli* cell fission. *Curr. Opin. Microbiol. 13*, 730−737.

(2) Lutkenhaus, J., Pichoff, S., and Du, S. (2012) Bacterial cytokinesis: From Z ring to divisome. *Cytoskeleton 69*, 778−790.

(3) Typas, A., Banzhaf, M., Gross, C. A., and Vollmer, W. (2012) From the regulation of peptidoglycan synthesis to bacterial growth and morphology. *Nat. Rev. Microbiol. 10*, 123−136.

(4) Arends, S. J., Williams, K., Scott, R. J., Rolong, S., Popham, D. L., and Weiss, D. S. (2010) Discovery and characterization of three new *Escherichia coli* septal ring proteins that contain a SPOR domain: DamX, DedD, and RlpA. *J. Bacteriol. 192*, 242−255.

(5) Gerding, M. A., Liu, B., Bendezu, F. O., Hale, C. A., Bernhardt, T. G., and de Boer, P. A. (2009) Self-enhanced accumulation of FtsN at division sites and roles for other proteins with a SPOR domain (DamX, DedD, and RlpA) in *Escherichia coli* cell constriction. *J. Bacteriol. 191*, 7383−7401.

(6) Moll, A., and Thanbichler, M. (2009) FtsN-like proteins are conserved components of the cell division machinery in proteobacteria. *Mol. Microbiol. 72*, 1037−1053.

(7) Finn, R. D., Mistry, J., Tate, J., Coggill, P., Heger, A., Pollington, J. E., Gavin, O. L., Gunasekaran, P., Ceric, G., Forslund, K., Holm, L., Sonnhammer, E. L., Eddy, S. R., and Bateman, A. (2010) The Pfam protein families database. *Nucleic Acids Res. 38*, D211−D222.

(8) Smith, T. J., and Foster, S. J. (1995) Characterization of the involvement of two compensatory autolysins in mother cell lysis during sporulation of *Bacillus subtilis* 168. *J. Bacteriol. 177*, 3855−3862.

(9) Ursinus, A., van den Ent, F., Brechtel, S., de Pedro, M., Holtje, J. V., Lowe, J., and Vollmer, W. (2004) Murein (peptidoglycan) binding property of the essential cell division protein FtsN from *Escherichia coli*. *J. Bacteriol. 186*, 6728−6737.

(10) Lupoli, T. J., Taniguchi, T., Wang, T. S., Perlstein, D. L., Walker, S., and Kahne, D. E. (2009) Studying a cell division amidase using defined peptidoglycan substrates. *J. Am. Chem. Soc. 131*, 18230−18231.

(11) de Pedro, M. A., Quintela, J. C., Holtje, J. V., and Schwarz, H. (1997) Murein segregation in *Escherichia coli*. *J. Bacteriol. 179*, 2823−2834.

(12) Ishidate, K., Ursinus, A., Holtje, J. V., and Rothfield, L. (1998) Analysis of the length distribution of murein glycan strands in *ftsZ* and *ftsI* mutants of *E. coli*. *FEMS Microbiol. Lett. 168*, 71−75.

(13) Obermann, W., and Holtje, J. V. (1994) Alterations of murein structure and of penicillin-binding proteins in minicells from *Escherichia coli*. *Microbiology 140* (Part 1), 79−87.

(14) Romeis, T., Kohlrausch, U., Burgdorf, K., and Holtje, J. V. (1991) Murein chemistry of cell division in *Escherichia coli*. *Res. Microbiol. 142*, 325−332.

(15) Mishima, M., Shida, T., Yabuki, K., Kato, K., Sekiguchi, J., and Kojima, C. (2005) Solution structure of the peptidoglycan binding domain of *Bacillus subtilis* cell wall lytic enzyme CwlC: Characterization of the sporulation-related repeats by NMR. *Biochemistry 44*, 10153−10163.

(16) Yang, J. C., Van Den Ent, F., Neuhaus, D., Brevier, J., and Lowe, J. (2004) Solution structure and domain architecture of the divisome protein FtsN. *Mol. Microbiol. 52*, 651−660.

(17) Allain, F. H., Howe, P. W., Neuhaus, D., and Varani, G. (1997) Structural basis of the RNA-binding specificity of human U1A protein. *EMBO J. 16*, 5764−5772.

(18) Birney, E., Kumar, S., and Krainer, A. R. (1993) Analysis of the RNA-recognition motif and RS and RGG domains: Conservation in metazoan pre-mRNA splicing factors. *Nucleic Acids Res. 21*, 5803−5816.

(19) Nagai, K., Oubridge, C., Jessen, T. H., Li, J., and Evans, P. R. (1990) Crystal structure of the RNA-binding domain of the U1 small nuclear ribonucleoprotein A. *Nature 348*, 515−520.

(20) Mosyak, L., Zhang, Y., Glasfeld, E., Haney, S., Stahl, M., Seehra, J., and Somers, W. S. (2000) The bacterial cell-division protein ZipA and its interaction with an FtsZ fragment revealed by X-ray crystallography. *EMBO J. 19*, 3179−3191.

(21) Fribourg, S., Gatfield, D., Izaurralde, E., and Conti, E. (2003) A novel mode of RBD-protein recognition in the Y14-Mago complex. *Nat. Struct. Biol. 10*, 433−439.

(22) Kadlec, J., Izaurralde, E., and Cusack, S. (2004) The structural basis for the interaction between nonsense-mediated mRNA decay factors UPF2 and UPF3. *Nat. Struct. Mol. Biol. 11*, 330−337.

(23) Varani, G., and Nagai, K. (1998) RNA recognition by RNP proteins during RNA processing. *Annu. Rev. Biophys. Biomol. Struct. 27*, 407−445.

(24) Lyngstadaas, A., Lobner-Olesen, A., and Boye, E. (1995) Characterization of three genes in the *dam*-containing operon of *Escherichia coli*. *Mol. Gen. Genet. 247*, 546−554.

(25) Lopez-Garrido, J., Cheng, N., Garcia-Quintanilla, F., Garcia-del Portillo, F., and Casadesus, J. (2010) Identification of the *Salmonella enterica damX* gene product, an inner membrane protein involved in bile resistance. *J. Bacteriol. 192*, 893−895.

(26) Leclerc, G. J., Tartera, C., and Metcalf, E. S. (1998) Environmental regulation of *Salmonella typhi* invasion-defective mutants. *Infect. Immun. 66*, 682−691.

(27) Ruiz, C., and Levy, S. B. (2010) Many chromosomal genes modulate MarA-mediated multidrug resistance in *Escherichia coli*. *Antimicrob. Agents Chemother. 54*, 2125−2134.

(28) Tarry, M., Arends, S. J., Roversi, P., Piette, E., Sargent, F., Berks, B. C., Weiss, D. S., and Lea, S. M. (2009) The *Escherichia coli* cell division protein and model Tat substrate SufI (FtsP) localizes to the septal ring and has a multicopper oxidase-like structure. *J. Mol. Biol. 386*, 504−519.

(29) Haldimann, A., and Wanner, B. L. (2001) Conditional-replication, integration, excision, and retrieval plasmid-host systems for gene structure-function studies of bacteria. *J. Bacteriol. 183*, 6384−6393.

(30) Ottiger, M., Delaglio, F., and Bax, A. (1998) Measurement of J and dipolar couplings from simplified two-dimensional NMR spectra. *J. Magn. Reson. 131*, 373−378.

(31) Ruckert, M., and Otting, G. (2000) Alignment of biological macromolecules in novel nonionic liquid crystalline media for NMR experiments. *J. Am. Chem. Soc. 122*, 7793−7797.

(32) Farrow, N. A., Muhandiram, R., Singer, A. U., Pascal, S. M., Kay, C. M., Gish, G., Shoelson, S. E., Pawson, T., Formankay, J. D., and Kay, L. E. (1994) Backbone dynamics of a free and a phosphopeptide-complexed Src homology-2 domain studied by ^{15}N NMR relaxation. *Biochemistry 33*, 5984−6003.

(33) Delaglio, F., Grzesiek, S., Vuister, G. W., Zhu, G., Pfeifer, J., and Bax, A. (1995) NMRPipe: A multidimensional spectral processing system based on UNIX pipes. *J. Biomol. NMR 6*, 277−293.

(34) Palmer, A. G., Rance, M., and Wright, P. E. (1991) Intramolecular motions of a zinc finger DNA-binding domain from Xfin characterized by proton-detected natural abundance ^{13}C heteronuclear NMR spectroscopy. *J. Am. Chem. Soc. 113*, 4371−4380.

(35) Vranken, W. F., Boucher, W., Stevens, T. J., Fogh, R. H., Pajon, A., Llinas, P., Ulrich, E. L., Markley, J. L., Ionides, J., and Laue, E. D. (2005) The CCPN data model for NMR spectroscopy: Development of a software pipeline. *Proteins 59*, 687−696.

(36) Lipari, G., and Szabo, A. (1982) Model-free approach to the interpretation of nuclear magnetic-resonance relaxation in macro-molecules. 1. Theory and range of validity. *J. Am. Chem. Soc. 104*, 4546−4559.

(37) Lipari, G., and Szabo, A. (1982) Model-free approach to the interpretation of nuclear magnetic-resonance relaxation in macro-molecules. 2. Analysis of experimental results. *J. Am. Chem. Soc. 104*, 4559−4570.

(38) Loria, J. P., and Cole, R. (2003) FAST-Modelfree: A program for rapid automated analysis of solution NMR spin-relaxation data. *J. Biomol. NMR 26*, 203−213.

(39) Mandel, A. M., Akke, M., and Palmer, A. G., III (1995) Backbone dynamics of *Escherichia coli* ribonuclease HI: Correlations with structure and function in an active enzyme. *J. Mol. Biol. 246*, 144−163.

(40) Schwieters, C. D., Kuszewski, J. J., and Clore, G. M. (2006) Using Xplor-NIH for NMR molecular structure determination. *Prog. Nucl. Magn. Reson. Spectrosc. 48*, 47−62.

(41) Schwieters, C. D., Kuszewski, J. J., Tjandra, N., and Clore, G. M. (2003) The Xplor-NIH NMR molecular structure determination package. *J. Magn. Reson. 160*, 65−73.

(42) DeLano, W. L. (2008) *The PyMOL Molecular Graphics System*, version 1.1, DeLano Scientific, San Carlos, CA.

(43) Pettersen, E. F., Goddard, T. D., Huang, C. C., Couch, G. S., Greenblatt, D. M., Meng, E. C., and Ferrin, T. E. (2004) UCSF Chimera: A visualization system for exploratory research and analysis. *J. Comput. Chem. 25*, 1605−1612.

(44) Shen, Y., Delaglio, F., Cornilescu, G., and Bax, A. (2009) TALOS plus: A hybrid method for predicting protein backbone torsion angles from NMR chemical shifts. *J. Biomol. NMR 44*, 213−223.

(45) Sass, H. J., Musco, G., Stahl, S. J., Wingfield, P. T., and Grzesiek, S. (2001) An easy way to include weak alignment constraints into NMR structure calculations. *J. Biomol. NMR 21*, 275−280.

(46) Laskowski, R. A., Rullmann, J. A. C., MacArthur, M. W., Kaptein, R., and Thornton, J. M. (1996) AQUA and PROCHECK-NMR: Programs for checking the quality of protein structures solved by NMR. *J. Biomol. NMR 8*, 477−486.

(47) Ashkenazy, H., Erez, E., Martz, E., Pupko, T., and Ben-Tal, N. (2010) ConSurf 2010: Calculating evolutionary conservation in sequence and structure of proteins and nucleic acids. *Nucleic Acids Res. 38*, W529−W533.

(48) Schleifer, K. H., and Kandler, O. (1972) Peptidoglycan types of bacterial cell walls and their taxonomic implications. *Bacteriol. Rev. 36*, 407−477.

(49) Glauner, B., Holtje, J. V., and Schwarz, U. (1988) The composition of the murein of *Escherichia coli. J. Biol. Chem. 263*, 10088−10095.

(50) Atrih, A., Bacher, G., Allmaier, G., Williamson, M. P., and Foster, S. J. (1999) Analysis of peptidoglycan structure from vegetative cells of *Bacillus subtilis* 168 and role of PBP 5 in peptidoglycan maturation. *J. Bacteriol. 181*, 3956−3966.

(51) Dai, K., Xu, Y., and Lutkenhaus, J. (1993) Cloning and characterization of *ftsN*, an essential cell division gene in *Escherichia coli* isolated as a multicopy suppressor of *ftsA12*(Ts). *J. Bacteriol. 175*, 3790−3797.

(52) Oubridge, C., Ito, N., Evans, P. R., Teo, C. H., and Nagai, K. (1994) Crystal structure at 1.92 Å resolution of the RNA-binding domain of the U1A spliceosomal protein complexed with an RNA hairpin. *Nature 372*, 432−438.

(53) Varani, L., Gunderson, S. I., Mattaj, I. W., Kay, L. E., Neuhaus, D., and Varani, G. (2000) The NMR structure of the 38 kDa U1A protein−PIE RNA complex reveals the basis of cooperativity in regulation of polyadenylation by human U1A protein. *Nat. Struct. Biol. 7*, 329−335.

(54) Larkin, M. A., Blackshields, G., Brown, N. P., Chenna, R., McGettigan, P. A., McWilliam, H., Valentin, F., Wallace, I. M., Wilm, A., Lopez, R., Thompson, J. D., Gibson, T. J., and Higgins, D. G. (2007) Clustal W and Clustal X version 2.0. *Bioinformatics 23*, 2947−2948.